84-1032

QUATERNION FEEDBACK FOR SPACECRAFT LARGE ANGLE MANEUVERS

Bong Wie* and Peter M. Barba**

Ford Aerospace & Communications Corporation
Palo Alto, California

Abstract

This paper presents the stability and control analysis for large angle feedback reorientation maneuvers using reaction jets. Strapdown inertial reference system provides spacecraft attitude changes in terms of quaternions. Reaction jets with pulse-width pulse-frequency modulation provide proportional control torques. The use of quaternions as attitude errors for large angle feedback control is investigated. Closed-loop stability analysis for the 3-axis maneuvers is performed using the Liapunov's stability theorem. Unique characteristics of the quaternion feedback are discussed for single-axis motion using a phase-plane plot. The practical feasibility of a 3-axis large angle feedback maneuver is demonstrated by digital simulations.

Introduction

In many future spacecraft missions, large angle reorientation/slew maneuvers will be required. Conventional single-axis small angle feedback controls may not be adequate for the 3-axis large angle maneuvers. Many open-loop schemes (for example, see [1, 2]) have been proposed for large angle maneuvers. The purely open-loop maneuvers do not require any measurement for feedback, thus, there is no possibility of the closed-loop instability. However, in practice, they are sensitive to the spacecraft parameter uncertainties and to the unexpected disturbances. In general, combination of feedforward/feedback controls are desirable.

In an earlier work, Mortensen [3, 4] suggested the use of Cayley-Rodriguez parameters and quaternions as attitude errors for large angle feedback control. He extended the conventional linear regulator concept to the case of 3-axis large angle motion. Hrastar [5] applied Mortensen's control logic to the large angle slew maneuver of an Orbiting Astronomical Observatory (OAO) spacecraft. Recently, similar feedback control logic was compared with the model-reference adaptive slew maneuver about the Euler axis [6].

In most of the slew maneuver studies, reaction wheels have been extensively used for torquing devices. The use of on-off reaction jets for slew maneuvers is also often required. The so-called "bang-off-bang" may be the most common maneuver profile using the on-off reaction jets. Rapid slew maneuver about the Euler axis using reaction jets has been investigated by D'Amario and Stubbs [7].

In general, it is necessary to know the spacecraft attitude at all times for feedback controls. The large angle orientation can be represented by direction cosine matrix, Euler angles, or by quaternions. Quaternions [8, 9], also called Euler parameters, allow the description of the spacecraft orientation in all possible attitudes. Quaternions have no inherent geometrical singularity as do Euler angles; there are no singularities in the kinematical differential equations as do Cayley-Rodriguez parameters; and successive rotations follow the quaternion multiplication rules. Moreover, quaternions are well-suited for onboard real time computation since only products and no trigonometric relations exist in the quaternion equations. Thus, spacecraft orientation is now commonly described in terms of quaternions (e.g., HEAO, space shuttle, and Galileo [10]).

This paper presents the stability and control analysis of 3-axis large angle feedback maneuvers for a spacecraft which has an onboard microprocessor and strapdown inertial reference system. The rate integrating gyros operate in a pulse rebalance loop to provide incremental angle changes to the quaternion integration algorithm. The spacecraft has also earth and sun sensors, but not star sensor. Nearly proportional control torques are provided by pulse-width pulse-frequency modulated reaction jets. The use of quaternions as attitude errors for large angle feedback control will be investigated. Characteristics of quaternion feedback will be discussed using phase-plane plot for single-axis motion. Closed-loop stability analysis of quaternion feedback will be performed by using Liapunov's stability theorem. The practical feasibility of the large angle feedback maneuver will be demonstrated by digital simulations.

Reorientation Maneuver Requirements

Future spacecraft systems may use an integrated high efficiency bi-propellant propulsion system for both apogee and perigee maneuvers thereby reducing space shuttle launch costs. The orbital maneuvers will then be performed in the 3-axis stabilized mode in order to control a spacecraft with high liquid mass-fraction.

One of the unique characteristics of this system is the non-spinning deployment from the space shuttle. Many current satellites, which are 3-axis stabilized in orbit, are spin-stabilized during orbit injection. Thus, they are deployed from the space shuttle as spin-stabilized. However, if the spacecraft is 3-axis stabilized by using gimballed main engine during perigee maneuver, then it may be beneficial to have non-spinning deployment from the shuttle. Reaction jets with 5-lb thrust level are being considered for 3-axis attitude control of the spacecraft shown in Fig. 1.

Index Category: Spacecraft Dynamics and Control

* Engineering Specialist, Systems Analysis Dept., Member AIAA

** Principal Engineer, Systems Analysis Dept., Member AIAA

Imperfect deployment could induce an initial tip-off rotational rate which may induce large angle tumbling motion, if it is not actively controlled. However, the reaction jets should be disabled until the spacecraft is separated from the space shuttle by 200 ft, due to the shuttle safety requirement. The coast period without an active attitude control is about 200 sec since the expected deployment rate is 1 ft/sec for the spacecraft considered in this paper. During this period, the spacecraft will coast with large attitude drift due to an initial deployment tip-off rate of 0.5 deg/sec in its transverse axes (negligible in longitudinal axis). The strapdown inertial reference system must track the spacecraft's attitude drift during this coast period. After being separated from the space shuttle by 200 ft, the reaction jets are enabled to reorient the spacecraft to its desired attitude. Thus, the spacecraft may require a large angle reorientation maneuver up to 180 degrees.

The perigee orbit injection maneuver requires a total velocity pointing error of ± 3 deg (3 sigma). Part of the pointing error is due to the attitude determination error which includes the bias and scale factor errors of the gyros and also the computational error of the strapdown attitude algorithm. The reorientation pointing requirement is allocated as ± 0.5 deg (3 sigma) which is mainly due to attitude determination errors. A functional block diagram for the attitude determination and control system is shown in Fig. 2.

Attitude Determination and Control

Consider the general case of a rigid spacecraft rotating under the influence of body-fixed torquing devices. The Euler equations of motion about the principal axes of inertia are:

$$I_1\dot{\omega}_1 + (I_3 - I_2)\omega_2\omega_3 = T_1 \tag{1a}$$

$$I_2\dot{\omega}_2 + (I_1 - I_3)\omega_1\omega_3 = T_2 \tag{1b}$$

$$I_3\dot{\omega}_3 + (I_2 - I_1)\omega_1\omega_2 = T_3 \tag{1c}$$

where $(\omega_1, \omega_2, \omega_3)$, (I_1, I_2, I_3), and (T_1, T_2, T_3) are the spacecraft angular rates, the moments of inertia, and the control torques about the principal axes, respectively.

Euler's rotational theorem states that the rigid body attitude can be changed from any given orientation to any other orientation by rotating the body about an axis, called the Euler-axis, that is fixed to the rigid body and stationary in inertial space. The quaternion then defines the spacecraft attitude as an Euler-axis rotation from an inertial reference frame. The four elements of quaternions are defined as:

$$Q_1 = C_1 \sin(\phi/2) \tag{2a}$$

$$Q_2 = C_2 \sin(\phi/2) \tag{2b}$$

$$Q_3 = C_3 \sin(\phi/2) \tag{2c}$$

$$Q_4 = \cos(\phi/2) \tag{2d}$$

where ϕ is the magnitude of the Euler-axis rotation and (C_1, C_2, C_3) are the direction cosines of the Euler axis relative to the inertial reference frame.

The kinematical differential equations for the quaternion are:

$$2\dot{Q}_1 = \omega_1 Q_4 - \omega_2 Q_3 + \omega_3 Q_2 \tag{3a}$$

$$2\dot{Q}_2 = \omega_1 Q_3 + \omega_2 Q_4 - \omega_3 Q_1 \tag{3b}$$

$$2\dot{Q}_3 = -\omega_1 Q_2 + \omega_2 Q_1 + \omega_3 Q_4 \tag{3c}$$

$$2\dot{Q}_4 = -\omega_1 Q_1 - \omega_2 Q_2 - \omega_3 Q_3 \tag{3d}$$

with the constraint equation of quaternion unit norm

$$Q_1^2 + Q_2^2 + Q_3^2 + Q_4^2 = 1$$

The initial condition of Q_i in Eq. (3) defines the initial spacecraft attitude w.r.t. the inertial reference frame. For example, initial quaternions of (0, 0, 0, 1) define that the spacecraft is initially aligned with the inertial reference frame.

For small attitude changes from the inertial reference frame ($Q_1 = Q_2 = Q_3 \cong 0$, $Q_4 \cong 1$), we have $2\dot{Q}_1 = \omega_1$, $2\dot{Q}_2 = \omega_2$, and $2\dot{Q}_3 \cong \omega_3$ from Eq. (3). Thus, the following approximations hold for small angles: $\theta_1 = 2Q_1$, $\theta_2 = 2Q_2$, and $\theta_3 = 2Q_3$ where $(\theta_1, \theta_2, \theta_3)$ are the conventional Euler angles. For a simple rotation about the fixed Euler-axis, we also have the relations: $\omega_1 = C_1\dot{\phi}$, $\omega_2 = C_2\dot{\phi}$, and $\omega_3 = C_3\dot{\phi}$ where C_1, C_2, and C_3 are constant direction cosines of the Euler-axis w.r.t. the inertial reference frame.

The quaternion kinematical differential equations are linear with time-varying coefficients for known body rates. They have repeated eigenvalues at

$$\pm j\sqrt{\omega_1^2+\omega_2^2+\omega_3^2}\,/2.$$

In other words, the quaternion equations are neutrally stable for any value of angular rate input. This property may cause some difficulty in the numerical integration of the quaternion equations. All explicit numerical methods which are suitable for real-time computation have stability boundaries that do not include the imaginary axis except the origin. Therefore, any truncation or roundoff errors introduced in the computation will, in general, not die out. The strapdown attitude algorithm to be implemented in the onboard microprocessor will be discussed later.

The quaternion feedback control laws to be considered in this paper are:

Control Law #1

$$T_1 = -T_c\,[\,Kq_1 + K_1\omega_1\,] \tag{4a}$$

$$T_2 = -T_c\,[\,Kq_2 + K_2\omega_2\,] \tag{4b}$$

$$T_3 = -T_c\,[\,Kq_3 + K_3\omega_3\,] \tag{4c}$$

Control Law #2

$$T_1 = -T_c \left[Kq_1/q_4^3 + K_1\omega_1 \right] \quad (5a)$$

$$T_2 = -T_c \left[Kq_2/q_4^3 + K_2\omega_2 \right] \quad (5b)$$

$$T_3 = -T_c \left[Kq_3/q_4^3 + K_3\omega_3 \right] \quad (5c)$$

Control Law #3

$$T_1 = -T_c \left[\text{sgn}(q_4)\, Kq_1 + K_1\omega_1 \right] \quad (6a)$$

$$T_2 = -T_c \left[\text{sgn}(q_4)\, Kq_2 + K_2\omega_2 \right] \quad (6b)$$

$$T_3 = -T_c \left[\text{sgn}(q_4)\, Kq_3 + K_3\omega_3 \right] \quad (6c)$$

where

$$\begin{bmatrix} q_1 \\ q_2 \\ q_3 \\ q_4 \end{bmatrix} = \begin{bmatrix} \bar{Q}_4 & \bar{Q}_3 & -\bar{Q}_2 & -\bar{Q}_1 \\ -\bar{Q}_3 & \bar{Q}_4 & \bar{Q}_1 & -\bar{Q}_2 \\ \bar{Q}_2 & -\bar{Q}_1 & \bar{Q}_4 & -\bar{Q}_3 \\ \bar{Q}_1 & \bar{Q}_2 & \bar{Q}_3 & \bar{Q}_4 \end{bmatrix} \begin{bmatrix} Q_1 \\ Q_2 \\ Q_3 \\ Q_4 \end{bmatrix} \quad (7)$$

where q_i is the control error quaternion, Q_i is the commanded attitude quaternion w.r.t. the inertial reference frame, $\bar{Q}_i$ is the currently estimated spacecraft quaternion w.r.t. the inertial reference frame, and T_c is the control torque level of reaction jets; K and K_i are positive control gains.

Eq. (7) is the result of successive quaternion rotations using the quaternion multiplication and inversion rules. The control error quaternion, q_i, is simply the current spacecraft attitude quaternion w.r.t. the commanded attitude. For a special case of attitude regulation w.r.t. the inertial reference frame, the commanded quaternion is (0, 0, 0, 1). Then, the currently estimated spacecraft quaternion simply becomes the control error quaternion. Also for an inertially-fixed commanded attitude quaternion, Q_i becomes the control error quaternion with re-initialization using Eq. (7).

The three control laws presented above are analogous to a conventional feedback control law in that the control torque is a function of position and rate. The first is linear feedback of state variables, while the second and third are nonlinear feedback control. The pulse-width pulse-frequency modulator was considered as a linear device in the above equations. The theoretical background of such assumption will be discussed later.

A Special Case of Single-Axis Large Angle Rotation

Some physical insight of the quaternion feedback control laws can be obtained by considering a single-axis large angle rotation. The closed-loop equations with the control laws #1, 2, and 3 can then be written as:

Control Law #1:

$$I\ddot{\phi} + T_c K_R \dot{\phi} + T_c K \sin(\phi/2) = 0 \quad (8a)$$

Control Law #2:

$$I\ddot{\phi} + T_c K_R \dot{\phi} + T_c K \sin(\phi/2)/\cos^3(\phi/2) = 0 \quad (8b)$$

Control Law #3:

$$I\ddot{\phi} + T_c K_R \dot{\phi} + T_c K \,\text{sgn}\left[\cos(\phi/2)\right] \sin(\phi/2) = 0 \quad (8c)$$

where ϕ is the single-axis attitude error, and attitude control about the origin is considered here.

We notice that the closed-loop equations have linear viscous damping and nonlinear "spring" terms. Eq. (8a) is similar to the nonlinear equation of a simple pendulum with viscous damping. Thus, the closed-loop behavior of the control law #1 is very much similar to the nonlinear behavior of a simple pendulum with large angle motion [17, 18].

A typical phase-plane plot of Eq. (8a) is shown in Fig. (3). Every trajectory, other than the separatrices going into the saddle points, ultimately approaches one of the stable equilibrium points. The number of full rotations before reaching the equilibrium point depends on the initial magnitude of rate. As to be expected, the greater the initial rate, the greater the number of full rotation before reaching the stable equilibrium point.

The separatrices come into the saddle points at $\phi = \pm 2\pi, \pm 6\pi, \ldots$, whereupon the spacecraft has the choice of rotating either in the same direction or backward. Such saddle points in Fig. (3) correspond to the upside down position of a simple pendulum problem (but with ϕ = 180 deg). The stable equilibrium points are $\phi = 0, \pm 4\pi, \ldots$ as can be seen from Eq. (8a). For the control law #1, the saddle points correspond to $Q_4 = -1$; the stable equilibrium points correspond to $Q_4 = 1$. It is important to note that both the saddle and stable points in Fig. 3 correspond to the physically identical orientation.

Similar phase-plane plots for Eqs. (8b) and (8c) can also be constructed, which have saddle points at $\phi = \pm\pi, \pm 3\pi, \ldots$ and stable equilibrium points at $\phi = 0, \pm 2\pi, \pm 4\pi, \ldots$ Simple phase-plane interpretation discussed here may be useful to gaining physical insight into 3-axis large angle motion.

Liapunov Nonlinear Stability Analysis

Closed-loop stability is the major concern in any feedback control system design. If the system is linear and time-invariant, many stability criteria are available. If the system is nonlinear, such stability criteria do not apply. For small angles, the system with the control laws discussed previously become the classical single-axis position and rate feedback, which is well-known to be closed-loop stable. For single-axis large angle motion, the stability can be easily studied using phase-plane plot, as discussed before. However, for 3-axis large angle motion, it is not obvious whether such control laws can provide global

closed-loop stability or not.

The Liapunov second method (also known as the Liapunov direct method) to be used in this paper may be the most general method for the determination of stability of nonlinear systems. By using the Liapunov second method, we can determine the stability of a system without solving the state equations. Only inertailly-fixed commanded attitude quaternion is considered here.

First, consider the control law #1. After substituting Eqs. (4) and (7) into the Euler equations, multiply each equation by ω_1, ω_2, and ω_3, respectively. After multiplying each equation of Eq. (3) by $T_cK(Q_1-\bar{Q}_1)$, $T_cK(Q_2-\bar{Q}_2)$, $T_cK(Q_3-\bar{Q}_3)$, and $T_cK(Q_4-\bar{Q}_4)$ respectively, add these equations to the previously modified Euler equations. We then have

$$\dot{V} = \sum_{i=1}^{3} I_i\dot{\omega}_i\omega_i + 2T_cK\sum_{i=1}^{4}\dot{Q}_i(Q_i-\bar{Q}_i) = -T_c\sum_{i=1}^{3}K_i\omega_i^2 < 0 \qquad (9)$$

A positive definitie Liapunov function, V, can then be found as

$$V = 1/2\sum_{i=1}^{3} I_i\omega_i^2 + T_cK\sum_{i=1}^{4}(Q_i - \bar{Q}_i)^2 > 0 \qquad (10)$$

Thus, the closed-loop system with the control law #1 is asymptotically stable in the large, since $\dot{V} < 0$, $\lim_{t\to\infty} V(x) = 0$ and $\lim_{\|x\|\to\infty} V(x)\to\infty$, where x is the state vector. The stable equilibrium point with this control law is: $\omega_1 = \omega_2 = \omega_3 = 0$ and $Q_i = \bar{Q}_i$ (i = 1, 2, 3, 4). Thus, this control law reorients the spacecraft to the desired attitude from an arbitrary initial orientation.

Similarly, for the control law #2, substitute Eqs. (5) and (7) into the Euler equations, then multiply each equation by $2\omega_1$, $2\omega_2$, and $2\omega_3$ respectively. Multiply each equation of Eq. (3) by $-T_cK(Q_i + 2\dot{Q}_i/q_4)$, i = 1, 2, 3, 4. Add these equations to the previously modified Euler equations, we then have

$$\dot{V} = 2\sum_{i=1}^{3} I_i\dot{\omega}_i\omega_i - 2T_cK\sum_{i=1}^{4}\dot{Q}_i(Q_i+\bar{Q}_i) + 2T_cK(1-2q_4^{-3})\dot{q}_4$$

$$= -2T_c\sum_{i=1}^{3}K_i\omega_i^2 < 0 \qquad (11)$$

A positive definitive Liapunov function, V, can then be found as

$$V = \sum_{i=1}^{3} I_i\omega_i^2 - T_cK\sum_{i=1}^{4}(Q_i+\bar{Q}_i)^2 + 2T_cK(q_4+q_4^{-2})$$

$$= \sum_{i=1}^{3} I_i\omega_i^2 + 2T_cK(-1+q_4^{-2}) > 0 \quad (\text{since } |q_4| \leq 1) \qquad (12)$$

Thus, the closed-loop system with the control law #2 is also asymptotically stable in the large, since $\dot{V} < 0$, $\lim_{t\to\infty} V(x) = 0$, $\lim_{\|x\|\to\infty} V(x)\to\infty$.

Note that there exist two asumptotically stable equilibirum points with the second control law: $Q_i = \pm\bar{Q}_i$, i = 1, 2, 3, 4. The equilibrium point with $Q_i = \bar{Q}_i$ is physically the same orientation with $Q_i = -\bar{Q}_i$. For an initial error of $q_4 < 0$, the second control law becomes positive position feedback; it provides a shorter path and least action to reach the desired equilibrium point.

For small angles, the three control laws provide the same linear performance. However, for large angles, they provide significantly different performances. The q_4 becomes zero as the Euler rotation angle, ϕ, becomes 180 degrees. Thus, the second control law can result in a nearly infinite control signal for certain initial orientations. The first control law, however, never results in such a situation since the magnitude of q_i (i = 1,2,3) is never greater than one. For an initial orientation with $q_4 < 0$, however, the second control law provides more efficient reorientation maneuvers as discussed before.

The 3rd control law provides an efficient reorientation maneuver for an arbitrary initial orientation without the possibility of an infinite control signal. Feedforward time-varying slew command can also be generated to achieve smooth and time- and/or fuel-optimal maneuvers. In this paper, we consider feedback reorientation maneuvers with simple step attitude change command; time-varying slew command [7, 16, 20] is not considered.

In the previous stability analysis, the position gain has been restricted to be the same in each axis. Such a restriction resulted in an easy determination of the Liapunov function. It doesn't mean that the control laws discussed before become unstable without such constraint. Asymptotic stability in the large has not yet been proven when different position gain is used in each axis. Although we can't conclude anything about global stability from the stability of linearized system, it is known that when a linearized system is asymptotically stable the nonlinear system from which it is derived is also asymptotically stable [17].

Consider the control law #1 with different position gain in each axis. When the closed-loop system is linearized near the equilibrium point, the result is three uncoupled linear second-order systems. These are easily proven asymptotically stable by conventional methods. Thus, the original nonlinear system is also asymptotically stable with different position gain in each axis.

For a special case of 3-axis large angle motion but with small angular rate, the global stability of the control laws (#1, 2, 3) with different position gain in each axis can also be easily proved by Liapunov stability theorem.

PWPF Modulator

The Pulse-Width Pulse-Frequency (PWPF) modulator has been assumed as a linear device in the previous analysis. In this section, the theoretical background of such assumption will be briefly discussed. The PWPF modulator shown in Fig. 4a produces a pulse command sequence to the thruster valve by adjusting the pulse width and pulse frequency. In the linear range, the average torque produced equals the demanded torque input. The pulse width is very short and the pulse frequency is usually fast compared ot the spacecraft rigid body dynamics.

The static characteristics of the modulator are good enough for rigid spacecraft attitude control, while the dynamic characteristics of the modulator are needed for flexible spacecraft attitude control, e.g., see Wie and Plescia [15].

With a constant input, the PWPF modulator drives the thruster valve with an on-off pulse sequence having a nearly linear duty cycle with input amplitude. The duty cycle or modulation factor is defined as the average output of the modulator. The static characteristics of the continuous-time modulator for a constant input E are as follows:

$$\text{Minimum Pulse Width} \cong T_m h/K_m U_m \tag{14a}$$

$$\text{Internal Deadband} \quad E_d = U_{on}/K_m \tag{14b}$$

$$\text{Saturation Level} \quad E_s = U_m + U_{off}/K_m \tag{14c}$$

where $h \triangleq U_{on} - U_{off}$ = hysterisis width.

The U_{on}, U_{off}, K_m, and T_m are the design parameters of the modulator. A typical plot of the duty cycle which is nearly linear over the range above deadband and below saturation is shown in Fig. 4b.

A discrete-time PWPF modulator for microprocessor implementation is also shown in Fig. 4c. The modulator gets an input signal every T sec and causes pulse command updates every T/4 sec. Equation (13a) derived for a continuous-time modulator becomes invalid for a discrete-time modulator. An equality relation for the discrete-time modulator with T/4 sec minimum pulse width can be obtained as

$$h < K_m U_m T/4T_m < 2U_{on} \tag{15}$$

where T is the microprocessor sampling period.

The modulator provides an effective loop gain reduction at lower frequency and additional phase lag at higher frequency. The phase lag of the modulator decreases as the time constant T_m decreases. Detailed describing function analysis of the modulator can be found from Ref. [15].

Quaternion Integration for Strapdown Inertial Reference

There are a number of numerical methods available for solving the quaternion equations. Methods which can be applied to the strapdown attitude algorithms include Taylor series expansion [5, 16], rotation vector concept [10-12], Runge-Kutta algorithms, and state transition matrix [13]. Of these methods, the Taylor series expansion lends itself well to the use of an incremental angle output from the digital rate integrating gyros.

The strapdown attitude algorithm using the 4th-order Taylor series expansion, which requires only the current information from the gyros can be written as [16]:

$$Q_i(t+T) = Q_i(t) + R_i(t) - D^2 Q_i(t)$$

$$\text{1st} \qquad \text{2nd}$$

$$- D^2 R_i(t)/3 + D^4 Q_i(t)/6 \tag{16}$$

$$\text{3rd} \qquad \text{4th-order}$$

where $D^2 = (\Delta\theta_1)^2 + (\Delta\theta_2)^2 + (\Delta\theta_3)^2$

$$R_1 = 1/2\ [\ \Delta\theta_1 Q_4 - \Delta\theta_2 Q_3 + \Delta\theta_3 Q_2\ ]$$

$$R_2 = 1/2\ [\ \Delta\theta_1 Q_3 + \Delta\theta_2 Q_4 - \Delta\theta_3 Q_1\ ]$$

$$R_3 = 1/2\ [-\Delta\theta_1 Q_2 + \Delta\theta_2 Q_1 + \Delta\theta_3 Q_4\ ]$$

$$R_4 = 1/2\ [-\Delta\theta_1 Q_1 - \Delta\theta_2 Q_3 - \Delta\theta_3 Q_4\ ]$$

and $\Delta\theta_1$, $\Delta\theta_2$, and $\Delta\theta_3$ are the incremental angle outputs from the gyros over the quaternion integration time step, T. The body rates to be used for feedback controls are simply $\Delta\theta_i/T$.

Different strapdown attitude algorithms can also be found from Refs. [10-12]. Such algorithms require the previous samples of the gyro outputs as well as the current ouptuts. For any algorithms there exist computational errors due to Taylor series truncation and microprocessor finite word length. Another type of error also exists known as degradation of quaternion unit norm length. However, this error can be eliminated by normalization of the quaternion update equation. Trade-off between algorithms complexity vs. algorithm truncation and roundoff errors is generally required.

Digital Simulation

A digital simulation was used to verify the practical feasibility of large angle feedback maneuvers. The spacecraft inertias are given in Fig. 1. The control torque level of reaction jets is assumed as 20 N-m in each axis, with negligible cross-axis coupling. The gyro has quantization of 0.9 arcsec/pulse, residual drift rate of 0.1 deg/hr, and scale factor error of 0.5%. It was assumed that only drift bias is estimated and calibrated in the shuttle before deployment. Thus, the scale factor error of 0.5% is relatively large and considered as the worst case. The 32-bit onboard microprocessor has 64 msec cycle time and 48 msec process delay.

The attitude determination error was defined as the difference between the true spacecraft attitude and the attitude computed from the strapdown inertial reference system using the gyros. Thus, the attitude errors consist of errors due to residual drift rate and scale factor error, and strapdown attitude update computational error. Because of a relatively fast sampling period of 64 msec, the pointing error is dominated by the gyro sensor error not by computational error. Thus, attitude update algorithm with the first-order Taylor was good enough for preliminary analysis and simulations. The true spacecraft attitude was computed by means of a 4th-order Runge-Kutta routine with integration time step of 16 msec in double precision.

The results of a typical simulation using the control law #1 are shown in Fig. 5 through 8. The desired attitude quaternion is assumed as (0, 0, 0, 1). The initial body rates are: $\omega_1 = \omega_2 = 0.53$ deg/sec and $\omega_3 = 0.053$ deg/sec. The control loop with K = 0.5 and $K_1 = 200$ is enabled at t = 200 sec. Thus, for the reorientation manevuer, the initial orientation is: $Q_1 = 0.685$, $Q_2 = 0.695$, $Q_3 = 0.153$, and $Q_4 = 0.153$ with Euler rotation angle of 162 deg.

The spacecraft quaternions shown in Fig. 5 approach the desired value in a well-behaved manner. Figure 6 shows the time histories of the

body rates and the Euler rotation angles. Note that the Euler rotation angle decreases in an exponential manner. Figure 7 shows the time histories of the jet-firings. The periods of acceleration and deceleration, and attitude hold are evident. The jet firings are acceptable in practical sense, although the maneuver was not "optimal" like an ideal "bang-off-bang". Total jet firing time was 50 sec during the 300-sec reorientation and 500-sec attitude hold mode. Figure 7 also shows some measure of spacecraft attitude determination error, which meets the pointing requirement of 0.5 deg after reorientation maneuver. The attitude determination error increases as the spacecraft attitude drifts due to the scale factor error. Once the control loop is closed (at t = 200 sec), the pointing error decreases with an offset error. The offset error is due to the different path between the coast and the reorientation. The attitude error increases very slowly as time goes on due to the gyro drift bias.

The attitude-hold mode with K = 100 and K_i = 200, which is automatically initiated at the end of the maneuver, maintains the attitude of the spacecraft inside the control loop deadband as shown in Fig. 8. The effective deadband angle was chosen as 0.1 degrees.

Conclusions

The stability and control analysis for large angle feedback reorientation maneuvers with strapdown inertial reference system have been presented. The control logic was a simple extension of the conventional feedback control to the 3-axis large angle coupled motion. Some physical interpretation of quaternion feedback was given using a phase-plane plot. Liapunov's stability theorem was used to determine the global stability of the closed-loop system. The maneuver discussed in this paper was not necessarily optimal in the theoretical sense of minimum time and/or fuel. However, the closed-loop system approached the desired attitude in a well-behaved manner. Dominant pointing error source was shown to be the effect of the gyro scale factor because of the nature of large-angle maneuvers.

References

1. Barba, P.M. and J.N. Aubrun, "Satellite Attitude Acquisition by Momentum Transfer," AIAA J. Vol. 14, No. 10, Oct., 1976.

2. Vadali, S.R. and J.L. Junkins, "Spacecraft Large Angle Rotational Maneuvers with Optimal Momentum Transfer," J. Astronautical Sciences, Vol. XXXI, No. 2, April-June, 1983.

3. Mortensen, R.E., "On Systems for Automatic Control of the Rotation of a Rigid Body," Electronics Research Lab., University of Calif. Berkeley, Rpt. No. 62-23, Nov. 27, 1963. (Also see J. Applied Mechanics, March 1965, pp. 228-230.)

4. Mortensen, R.E. "A Globally Stable Linear Attitude Regulator," International Journal of Control, Vol. 8, No. 3, pp. 297-302, 1968.

5. Hrastar, J., "Attitude Control of a Spacecraft with a Starpdown Inertial Reference System and Onboard Computer," NASA TN D-5959, Sept. 1970.

6. Bosch, P.P.J van den, et al., "An Adaptive Attitude Control System for Large Angle Slew Maneuvers," IFAC Automatic Control in Space, Netherland, 1982.

7. D'Amario, L.A. and G.S. Stubbs, "A New Single-Axis Autopilot for Rapid Spacecraft Attitude Maneuvers," J. Guidance and Control, Vol. 2, No. 4, July-Aug., 1979.

8. Margulies, G., "On Real Four-Parameter Representations of Satellite Attitude Motions," Mathematical Analysis Dept., Report No. 52, Philco Western Lab., Sept. 1963.

9. Kane, T.R., P.W. Likins, and D.A. Levinson, Spacecraft Dynamics, McGraw-Hill Book Company, 1983.

10. Wong, E.C. and W.G. Breckenridge, "Inertial Attitude Determination for a Dual-Spin Planetary Spacecraft," J. Guidance, Control and Dynamics, Vol. 6, No. 6, Nov.-Dec. 1983.

11. Miller, R.B., "A New Strapdown Attitude Algorithm," J. Guidance, Control and Dynamics, Vol. 6, No. 4, July-Aug. 1983.

12. McKern, R. and H. Musoff, "Strapdown Attitude Algorithms from a Geometric Viewpoint," J. Guidance and Control, Vol. 4, No. 6, Nov-Dec, 1981.

13. Mayo, R.A., "Relative Quaternion State Transition Relation," J. Guidance and Control, Vol. 2, No. 1, Jan.-Feb. 1979.

14. Bryson, A.E., Jr., Stabilization and Control of Flight Vehicles, Class Notes, Aero/Astro Dept., Stanford University, Stanford, CA., 1983.

15. Wie, B. and C.T. Plescia, "Attitude Stabilization of Flexible Spacecraft During Stationkeeping Maneuvers," AIAA Guidance and Control Conf., No. 83-2226, Gatlinburg, TN., Aug. 1983. (To be published in J. Guidance, Control and Dynamics).

16. Cunningham, D.C. et al., "System Design of the Annualar Suspension and Pointing System (ASPS)," AIAA G & C Conf., No. 78-1311, Palo Alto, CA., 1978.

17. Struble, R.A., Nonlinear Differential Equations, McGraw-Hill Book Company, 1962. pp. 131-136.

18. Cannon, R.H., Dynamics of Physical Systems, McGraw-Hill Book Company, 1967. pp 355-370.

19. Ickes, B.P., "A New Method for Performing Control System Attitude Computation Using Quaternions," AIAA Journal, Vol. 8, No. 1, January 1970.

20. Breckenridge, W.G. and G.K. Man, "Quaternions for Galileo Scan Platform Control," AAS/AIAA Astrodynamics Specialist Conference Paper No. 83-321, Lake Placid, New York, Aug. 22-25, 1983.

21. Floyd, M.A. et al., "Implementation of a Minimum Time and Fuel On/Off Thruster Control System for Flexible Spacecraft," AAS/AIAA Astrodynamics Specialist Conference Paper No. 83-376, Lake Placid, New York, Aug. 22-25, 1983.

SPACECRAFT DEPLOYMENT FROM SPACE SHUTTLE

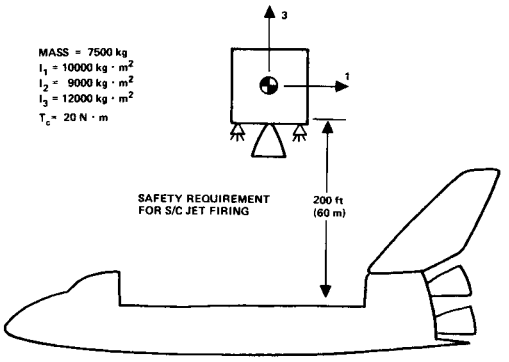

Figure 1.

ATTITUDE DETERMINATION AND CONTROL

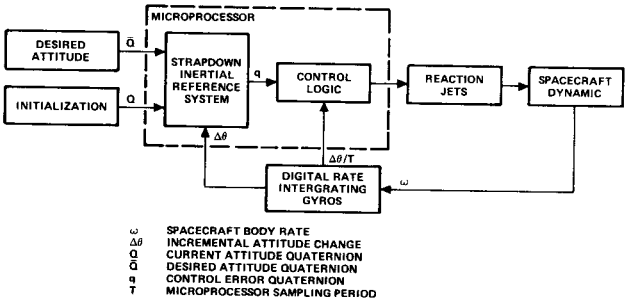

Figure 2.

PHASE-PLANE PLOT FOR SINGLE-AXIS ROTATION

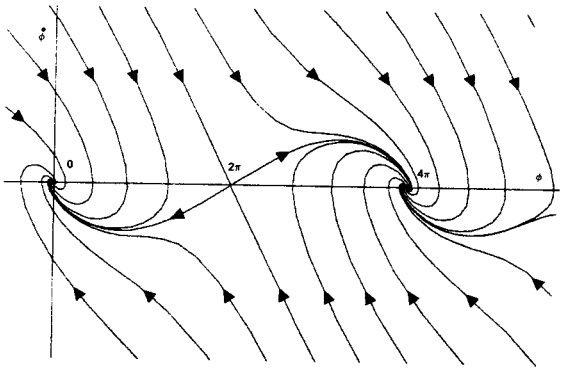

Figure 3.

PWPF MODULATOR

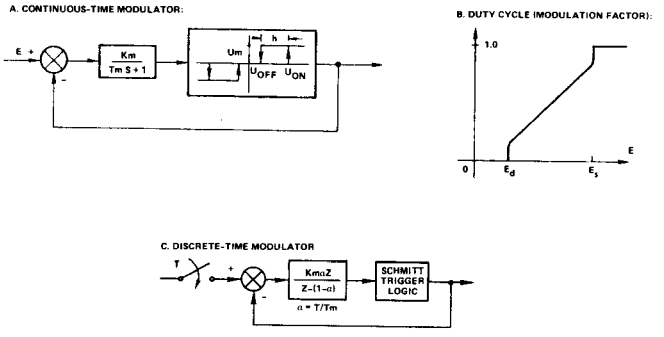

Figure 4.

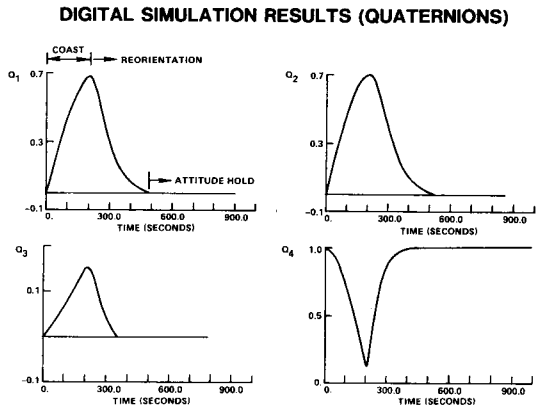

Figure 5.

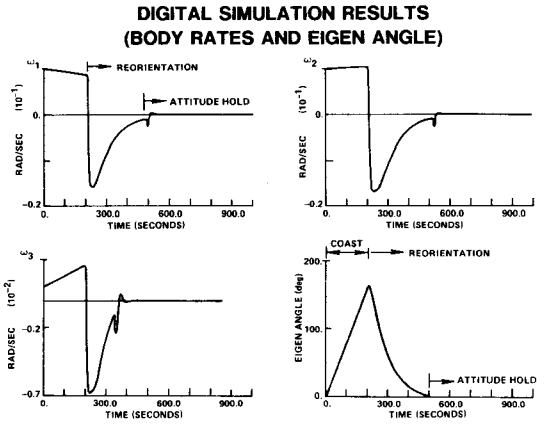

Figure 6.

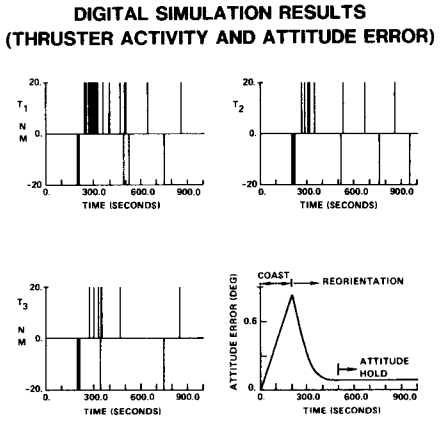

Figure 7.

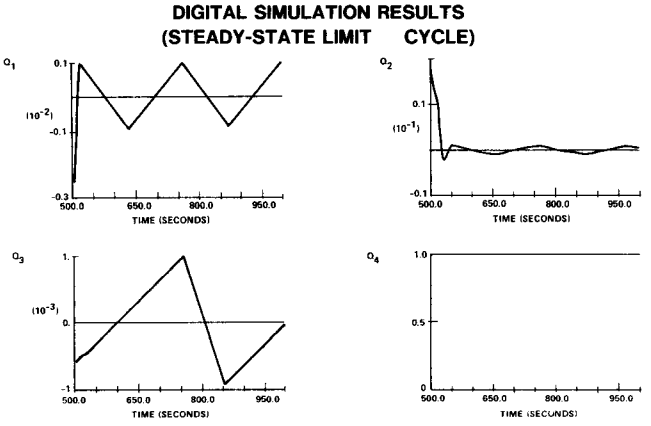

Figure 8.